Finite-Element Model Updating and Probabilistic Analysis of Timber-Concrete Composite Beams

Alessandro Zona, Ph.D., A.M.ASCE[1]; Michele Barbato, Ph.D., A.M.ASCE[2]; and Massimo Fragiacomo, Ph.D.[3]

Abstract: Timber-concrete composite beams are an increasingly common design solution for medium-to-long span floors in new buildings. Thus, there is a significant need for accurate models and analysis tools to predict the response and performance of timber-concrete composite beams. In this paper, a nonlinear finite-element (FE) frame model with deformable shear connection is adopted to estimate the short-term structural response of timber-concrete composite beams for which experimental results are available. The FE model is used in conjunction with a probabilistic analysis methodology, which explicitly accounts for the uncertainties in the parameters that describe the constitutive models for timber, concrete, and shear connectors. The objectives of this study are (1) the evaluation of the variability of global and local structural response quantities owing to the uncertainties in the constitutive parameters of timber, concrete, and shear connectors; and (2) the analysis of the correlation between experimental measurements and numerical results based on FE models in which the values of the constitutive parameters are set equal to their experimentally identified mean values and in which the values of the constitutive parameters are optimized through FE model updating, respectively. The results presented in this study show that uncertainties in the constitutive parameters of timber, concrete, and shear connectors have a significant influence on the correlation between the experimental and numerical results. In addition, the optimal values of material parameters obtained using the FE model updating procedure may show substantial variations with respect to the parameters' mean values as identified in the experimental testing. Prospective developments directed toward design applications and based on the obtained results are also discussed. **DOI: 10.1061/(ASCE)ST.1943-541X.0000509.**

CE Database subject headings: Timber construction; Composite beams; Finite element method; Nonlinear analysis; Probability distribution.

Author keywords: Timber construction; Composite beams; Finite element method; Nonlinear analysis; Probability distribution.

Introduction

Timber-concrete composite beams are made of a timber joist/beam connected to a concrete topping through an appropriate shear connection (Ceccotti 2002). This technique, originally developed for upgrading existing timber floors, is currently also proposed as a possible solution for medium-to-long span floors in new buildings. The concrete topping significantly increases the stiffness, with advantages in terms of reduced deflection and susceptibility to vibrations compared with timber-only floors. The concrete topping also improves the acoustic separation and thermal mass and increases the fire resistance and the load-carrying capacity of the composite system. In addition, the use of timber to replace the lower cracked part of a solid reinforced concrete floor ensures significant weight reduction with the following benefits: less load imposed on foundations, smaller seismic actions, and a more sustainable form of construction with less embodied energy and fewer CO_2 emissions (Yeoh et al. 2011c).

Extensive experimental research has been conducted on various timber-concrete composite systems, including fully prefabricated systems (Bathon et al. 2006; Lukaszewska et al. 2010), semiprefabricated systems (Yeoh et al. 2011a), and systems with cast-in situ concrete topping (Dias et al. 2007; Gutkowski et al. 2008). Various wood-based materials have been used, such as sawn timber, glue-laminated timber, and laminated veneer lumber (LVL). Several experimental programs that involve tests to failure in the short term (Gutkowski et al. 2008; Lukaszewska et al. 2010; Yeoh et al. 2011a), tests under repeated loads (Balogh et al. 2008), and long-term tests under sustained load (Ceccotti et al. 2007; To et al. 2011; Gutkowski et al. 2011) have demonstrated the overall good performance of the composite system over time. A key component is the shear connection, for which numerous solutions are available, such as glued or screwed mechanical connectors and notches cut in the timber and filled with concrete (Yeoh et al. 2011c). Mechanical connectors are more flexible and, therefore, less effective; notches are, conversely, stiffer. Because the case of full composite action in which there is no relative slip between concrete and timber is hardly achievable, it is important to take into account the flexibility of the connection system.

Various numerical models for short- and long-term analyses of timber-concrete composite beam have been developed, including analytical models based on the finite-difference method (FDM) (Schänzlin 2003), unidimensional (frame) finite-element (FE) models that account for the connection flexibility (Fragiacomo 2005;

[1]Assistant Professor, School of Architecture and Design, Univ. of Camerino, Viale della Rimembranza, 63100 Ascoli Piceno, Italy. E-mail: alessandro.zona@unicam.it

[2]Assistant Professor, Dept. of Civil and Environmental Engineering, Louisiana State Univ. at Baton Rouge, 3531 Patrick F. Taylor Hall, Nicholson Extension, Baton Rouge, LA 70803 (corresponding author). E-mail: mbarbato@lsu.edu

[3]Associate Professor, Dept. of Architecture, Design and Urban Planning, Univ. of Sassari, Palazzo del Pou Salit, Piazza Duomo 6, 07041 Alghero, Italy. E-mail: fragiacomo@uniss.it

Note. This manuscript was submitted on February 19, 2011; approved on September 23, 2011; published online on September 26, 2011. Discussion period open until December 1, 2012; separate discussions must be submitted for individual papers. This paper is part of the ***Journal of Structural Engineering***, Vol. 138, No. 7, July 1, 2012. ©ASCE, ISSN 0733-9445/2012/7-899–910/$25.00.

Fragiacomo and Ceccotti 2006), and three-dimensional FE models (To et al. 2011). Specifically, the experimental-numerical comparisons presented in the literature demonstrate the good approximation that is achievable using frame models (Fragiacomo 2006; Yeoh et al. 2011a).

To date, the aforementioned models have only been used for deterministic analyses of timber-concrete composite beams. However, loading conditions, material properties, geometry, and several other parameters often show considerable variability because they are stochastic quantities in nature. Modern design codes often directly account for parameter and model uncertainties with approximate procedures and underline the importance of assessing such uncertainties to ensure satisfactory designs (Melchers 1999). Thus, in addition to accurate deterministic models, a methodology is needed to propagate uncertainties from the parameters defining the model of the structure to the structural response quantities of interest to engineers. From an engineering viewpoint, probabilistic response analysis becomes particularly important for structures in which uncertainties are significant, such as in the case of timber and timber-concrete composite structures.

In this paper, a nonlinear FE beam model with a deformable shear connection is adopted to estimate the short-term structural response of LVL-concrete composite beams for which experimental results up to failure, as well as tests on specimens of LVL, concrete, and connectors, are available. The FE model is used in conjunction with a probabilistic analysis methodology, which explicitly accounts for the uncertainties in the parameters that describe the constitutive models for timber, concrete, and shear connectors. This study has two objectives. The first objective is the evaluation of the variability of global and local structural response quantities owing to the uncertainties in the constitutive parameters of timber, concrete, and shear connectors. This variability evaluation provides insight into the effects of model parameter uncertainty on the short-term structural response and performance of timber-concrete composite beams. The second objective is the analysis of the correlation between experimental measurements from beam tests and numerical results based on the FE models in which the values of the constitutive parameters are set equal to their mean values, as identified in experimental testing, and in which the values of the constitutive parameters are optimized through the FE model updating procedure, respectively. This analysis is crucial to validate the FE model (adequate representation of the major structural behavior aspects) and the experimental identification of the material parameters (adequate characterization of the material parameters through laboratory tests on materials and connectors). In this paper, to discuss the aforementioned issues, selected global and local numerical response results obtained from FE probabilistic response analysis and FE model updating of timber-concrete composite beams are illustrated and compared with the experimentally measured results obtained from beam tests.

Deterministic and Probabilistic Analysis of Timber-Concrete Composite Beams

Deterministic FE Response Analysis

In this study, timber-concrete composite beams are modeled using the Newmark et al. (1951) composite beam model with a deformable shear connection, originally introduced for steel-concrete composite beams. In this model, the Euler–Bernoulli beam theory (in small deformations) applies to both components of the composite beam, and the deformable shear connection is represented by an interface model with a continuously distributed bond,

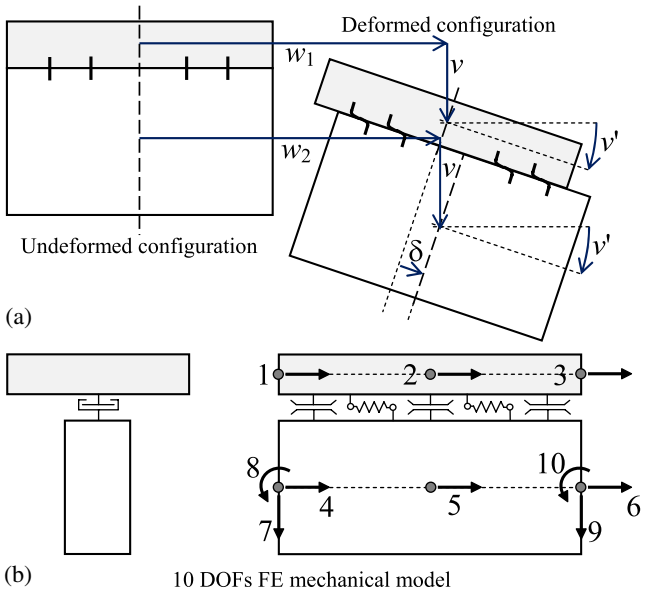

Fig. 1. Composite beam model: (a) kinematics; (b) 10-DOF FE with relevant displacement DOFs

allowing interlayer slip and enforcing contact; i.e., equal vertical deflection and rotation between the timber and concrete components [Fig. 1(a)].

The timber is modeled using an elasto-plastic constitutive law with assigned ultimate strain in compression and an elastic-brittle constitutive law in tension (Edlund 1995). The selected constitutive law for the concrete material in compression is the Saenz (1964) uniaxial law with zero strength in tension. The reinforcement steel is modeled using an elasto-plastic constitutive law with assigned ultimate strain. The shear connection is modeled using the following relationship experimentally derived by Ollgaard et al. (1971):

$$p_s = \text{sgn}(\delta) \cdot p_{s,\max} \cdot (1 - e^{-\beta \cdot |\delta|})^{\alpha}; \qquad \max(|\delta|) \le \delta_u \qquad (1)$$

where δ = slip between the two components of the composite beam; p_s = value of the shear force corresponding to δ; $p_{s,\max}$ = connection shear strength; α and β = parameters controlling the stiffness (slope of the curve) for small and intermediate (of the order of β^{-1}) values of the slip, respectively, as shown in Fig. 2; δ_u = ultimate slip; and sgn(…) = sign function.

The resulting nonlinear structural response problem is solved by using a dedicated FE code developed by Zona (2002), based

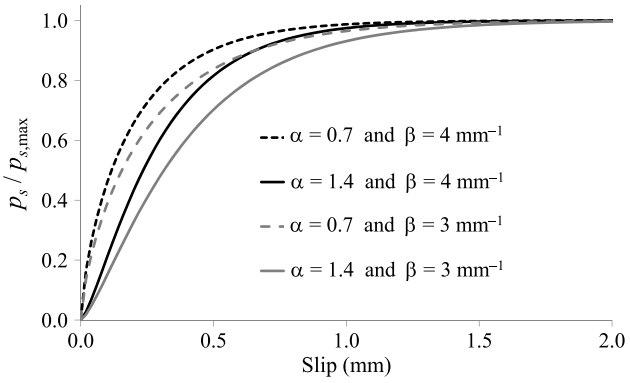

Fig. 2. Shear force versus slip from the Ollgaard et al. (1971) model for various values of the constitutive parameters α and β

on a 10 nodal degrees-of-freedom (DOFs) displacement-based composite frame element with a deformable shear connection [Fig. 1(b)]. Of the 10 DOFs, 8 DOFs are external (4 DOFs per end node) and 2 DOFs are internal (axial displacements of the timber beam and of the concrete slab, respectively), as shown in Fig. 1(b). This frame FE is the simplest displacement-based element for composite beams with deformable shear connection that avoids the eccentricity issue and the slip locking (Dall'Asta and Zona 2004), and has been widely adopted for nonlinear analysis of steel-concrete composite beams and frames (Dall'Asta and Zona 2002, 2005; Fragiacomo et al. 2004; Zona et al. 2008; Zona and Ranzi 2011), as well as for long-term analysis of timber-concrete composite beams (Fragiacomo 2005; Fragiacomo and Ceccotti 2006).

FE Response Sensitivity Analysis

FE response sensitivity analysis provides the gradient of the response quantities $\mathbf{r} = [r_1, r_2, \ldots, r_m]^T$ (where the superscript T denotes the vector/matrix transpose operator) with respect to the parameters $\boldsymbol{\theta} = [\theta_1, \theta_2, \ldots, \theta_n]^T$; i.e., $[\nabla_{\boldsymbol{\theta}}\mathbf{r}]_{ij} = \partial r_i/\partial\theta_j$, in which $i = 1, 2, \ldots, m$ and $j = 1, 2, \ldots, n$. The components of this gradient are called FE response sensitivities. FE response sensitivity analysis is used in several subfields of structural engineering, such as in FE model updating and simplified FE probabilistic response analysis, both of which are considered in this paper.

Several methods are available for computing FE response sensitivities, such as the FDM and the direct differentiation method (DDM) (Kleiber et al. 1997). The FDM consists of performing multiple FE response analyses by perturbing the value of the sensitivity parameter $\theta_i (i = 1, \ldots, n)$ by a small but finite amount $\Delta\theta_i$ in addition to a FE analysis with all parameters $\boldsymbol{\theta}$ set at their nominal values. Each response sensitivity is then calculated as the ratio between the response variation and the parameter perturbation. This method is computationally expensive and approximate in nature (Haftka and Gurdal 1993; Conte et al. 2003; Zona et al. 2005). The DDM consists of (1) differentiating analytically the discretized equations of equilibrium of the FE model for the considered structural system and (2) solving the obtained sensitivity equations as the FE analysis proceeds (Kleiber et al. 1997; Conte et al. 2003, 2004; Haukaas and Der Kiureghian 2004, 2005; Barbato and Conte 2005; Barbato et al. 2007). Thus, the DDM provides exact response sensitivities (consistent with the numerical response) at a small fraction of the computational cost of the additional FE analyses required by the FDM to obtain approximate response sensitivities (Conte et al. 2003; Haukaas and Der Kiureghian 2005). A detailed derivation of the DDM procedure for the 10-DOF FE models of composite beams with a deformable shear connection used in this study is available in Zona et al. (2005, 2006).

FE Model Updating

FE model updating consists of correcting the initial FE model by matching (up to a specified accuracy level) the structural response numerically obtained from the FE model with available experimental data (Zhang et al. 2001; Zivanovic et al. 2007). Owing to simplified mechanical models—as well as to incomplete knowledge and/or statistical uncertainty in the material, geometric, and other mechanical parameters characterizing the structural systems—a FE model based on the initial estimates of these model parameters may be unable to represent the behavior of the actual system with the level of accuracy required for a specific application. The final result of FE model updating is an updated FE model that can represent the mechanical behavior of the considered structural system with higher fidelity.

Two general classes of methods are used in FE model updating; i.e., direct methods and sensitivity-based methods (Friswell and Mottershead 1995). Direct methods update the global stiffness, damping, and/or mass matrices that appear in the structural equations of motion of the system under study (Baruch 1982; Wei 1990). However, these methods can lead to FE models with nonphysical values of some parameters or with different structural connectivities (Jaishi et al. 2007). Sensitivity-based methods use FE response sensitivities to adjust a preselected set of physical parameters and to minimize an objective function that represents the discrepancy between the computed and measured structural responses. A comprehensive survey of the earlier research on the topic can be found in Mottershead and Friswell (1993).

In this paper, nonlinear FE model updating is used to update the model parameters needed to define the nonlinear material constitutive models for timber, concrete, reinforcing steel and the shear connection in timber-concrete composite beams. This study adopts a sensitivity-based method that uses the sensitivities of FE global response quantities (e.g., deflection at midspan and external load) with respect to the material parameters of interest. The objective function, F, considered here is the sum of the squares of the difference between the numerically simulated and the experimentally recorded response at each load increment:

$$F(\boldsymbol{\theta}) = \sum_{i=1}^{N_{\text{step}}} [u_i(\boldsymbol{\theta}) - u_{i,\text{exp}}]^2 \tag{2}$$

in which u_i = numerically simulated midspan deflection at load increment i; $u_{i,\text{exp}}$ = experimentally recorded midspan deflection at load increment i; and N_{step} = total number of load increments. In Eq. (2), the dependency of the various quantities on the material parameters $\boldsymbol{\theta}$ is explicitly shown. The values of the material parameters are constrained to physically meaningful values. The constrained minimization of F is performed by using the MATLAB (MathWorks 2010a) function "fmincon" (MathWorks 2010b), whereas the FE response and response sensitivities needed at each iteration of the optimization process are computed using the dedicated FE code developed by Zona (2002), directly controlled through MATLAB.

Probabilistic FE Response Analysis

Probabilistic response analysis consists of computing the probabilistic characterization of the response of a structure given the probabilistic characterization of its input random parameters. Several methods are available for probabilistic response analysis (Melchers 1999); e.g., Monte Carlo simulation (MCS) and the first-order second-moment (FOSM) method (Haukaas and Der Kiureghian 2004; Barbato et al. 2010; Zona et al. 2010). MCS is a general and robust methodology. However, it requires knowledge of statistical information that, in general, is only partially available, and it could require a very large number of response analyses to obtain accurate estimates of the statistical moments of the response vector $\mathbf{R}$. The mean-centered FOSM method consists in estimating the first- and second-order statistical moments (mean values collected in the vector $\boldsymbol{\mu}_{\mathbf{R}}$, as well as variances and covariances collected in the matrix $\boldsymbol{\Sigma}_{\mathbf{R}}$) of $\mathbf{R}$ using its first-order Taylor series expansion in the random parameters $\boldsymbol{\Theta}$ about their mean values $\boldsymbol{\mu}_{\boldsymbol{\Theta}}$:

$$\mathbf{R}(\boldsymbol{\Theta}) \approx \mathbf{R}_{\text{lin}}(\boldsymbol{\Theta}) = \mathbf{r}(\boldsymbol{\mu}_{\boldsymbol{\Theta}}) + \nabla_{\boldsymbol{\theta}}\mathbf{r}|_{\boldsymbol{\theta}=\boldsymbol{\mu}_{\boldsymbol{\Theta}}} \cdot (\boldsymbol{\Theta} - \boldsymbol{\mu}_{\boldsymbol{\Theta}}) \tag{3}$$

where $\mathbf{r}$ = specific realization of the random quantity $\mathbf{R}$, and $\nabla_{\boldsymbol{\theta}}\mathbf{r}|_{\boldsymbol{\theta}=\boldsymbol{\mu}_{\boldsymbol{\Theta}}}$ = response sensitivities computed at the mean values, $\boldsymbol{\theta} = \boldsymbol{\mu}_{\boldsymbol{\Theta}}$, of the random structural parameters. Thus, the

first- and second-order statistical moments of $\mathbf{R}$ are approximated as follows (Barbato et al. 2010; Zona et al. 2010):

$$\boldsymbol{\mu}_{\mathbf{R}} \approx \boldsymbol{\mu}_{\mathbf{R}_{\text{lin}}} = \mathbf{r}(\boldsymbol{\mu}_{\boldsymbol{\Theta}}) \tag{4}$$

$$\boldsymbol{\Sigma}_{\mathbf{R}} \approx \boldsymbol{\Sigma}_{\mathbf{R}_{\text{lin}}} = \nabla_{\boldsymbol{\theta}}\mathbf{r}|_{\boldsymbol{\theta}=\boldsymbol{\mu}_{\boldsymbol{\Theta}}} \cdot \boldsymbol{\Sigma}_{\boldsymbol{\Theta}} \cdot (\nabla_{\boldsymbol{\theta}}\mathbf{r}|_{\boldsymbol{\theta}=\boldsymbol{\mu}_{\boldsymbol{\Theta}}})^T \tag{5}$$

where $\boldsymbol{\Sigma}_{\boldsymbol{\Theta}}$ = covariance matrix of $\boldsymbol{\Theta}$, determined when the standard deviations and the correlation coefficients of the random parameters are known. The FOSM method requires statistical information usually available (i.e., mean values, standard deviations, and correlation coefficients of the random parameters) and has a low additional computational cost compared with a deterministic-only response analysis. In addition, when structural response nonlinearities are in the low-to-moderate range, the FOSM approximation has been found to be sufficiently accurate in estimating the mean and standard deviations of response quantities for random structural systems under quasi-static loads (Barbato et al. 2010). Based on the aforementioned considerations, the FOSM method is validated through a comparison with MCS results and used as an efficient and practical technique for probabilistic analysis of timber-concrete composite structures.

Case Study: LVL-Concrete Composite Beams Tested in New Zealand

Description of the Beam Specimens and Experimental Setup

An extensive experimental program on LVL-concrete composite beams was undertaken at the University of Canterbury, Christchurch, New Zealand. This program included tests to failure under monotonic load of 11 full-scale strips of composite floor (Yeoh et al. 2011a), 13 small LVL-concrete composite blocks (push-out tests) to characterize the connection systems used in the beams (Yeoh et al. 2011b), and several concrete cubes and cylinders to characterize the mechanical properties of the concrete (Yeoh 2010). The beam specimens differed in span length (8 and 10 m), type of shear connection (large and small rectangular notches reinforced with a lag screw, as well as toothed metal plates), number of connectors along the beam length, and type of concrete (normal or with reduced shrinkage). The timber used was LVL manufactured by a New Zealand producer, which also provided the results of the quality control tests performed in the factory for the LVL batch used in the beam specimens constructed at the University of Canterbury.

Fig. 3 displays the experimental setup used in the four-point bending test to failure of the various beams. All relevant quantities, such as midspan deflection, relative slip at the connector location, and strains in the timber and concrete at midspan, were monitored during the tests. Two of the beam specimens tested at the University of Canterbury are used as benchmark problems in this study. These specimens are denoted as Beam E1 and Beam F1 and are characterized by notched and toothed metal plate connectors, respectively (Fig. 4). Beam E1 was made of one 400×63 mm LVL joist, 10 m long, connected with six connectors to a 65×600 mm concrete slab reinforced with a steel mesh $1\phi10$ at 200 mm c/c poured above a 17 mm plywood formwork. The connector was obtained by cutting a 50×300 mm rectangular notch in the LVL joist, which was then filled by concrete once the slab was poured (Fig. 5). A 16-mm-diameter lag screw was inserted in the timber at the center of the notch to reinforce it and improve the strength and post-peak behavior. Beam F1 had two 400×63 mm LVL joists, 8 m long, connected with eight connectors to a $65 \times 1{,}200$ mm concrete slab with the same reinforcement as in Beam E1. Each connector was made of two 136×333 mm toothed metal plates, one pressed in one LVL joist and the other in the other LVL joist, so that the two metal plates were between the two LVL joists (Fig. 5). The metal plates had several round openings in the upper part to allow a good bond and embedment in the concrete slab. More details can be found in Yeoh et al. (2011b).

Characterization of the Material Parameters of the LVL

Statistical information on the bending strength, f_b, or modulus of rupture (MOR), and on the apparent modulus of elasticity (MOE), E_b, of the LVL used in the timber component of the composite beams tested at the University of Canterbury was provided by the New Zealand LVL producer. It is noteworthy that the apparent MOE also includes an allowance for shear deformation. Mean values (μ), coefficients of variation (COVs), and correlation coefficients (ρ) are computed from 643 control tests on 95×63-mm LVL cross sections taken from entire billets of LVL. The following values are obtained: $\mu_{f_b} = 58.43$ MPa, $\text{COV}_{f_b} = 10.99\%$, $\mu_{E_b} = 11.53$ GPa, $\text{COV}_{E_b} = 7.59\%$, and $\rho_{f_b E_b} = 0.59$. Because the actual size of the LVL used in the composite beam specimens is 400×63 mm, the values given previously need to be corrected for the size effect. This correction is done using an experimentally derived strength reduction factor developed by the New Zealand LVL producer, fitted to the experimental results of bending tests on various LVL sizes. A strength reduction factor of 0.8016 from the 95×63-mm control specimens is obtained for the 400×63-mm specimens. Thus, the corrected mean value of the bending strength is $\mu_{f_b} = 46.84$ MPa.

Statistical information on the tensile strength, f_t, was also provided by the New Zealand LVL producer. In this case, the strength value depends on the length of the specimen tested and reduces as

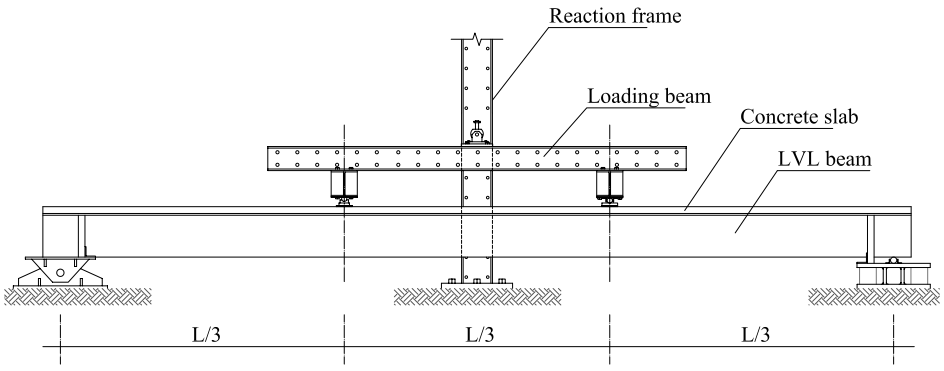

Fig. 3. Experimental setup of the tests to failure (data from Yeoh et al. 2011a)

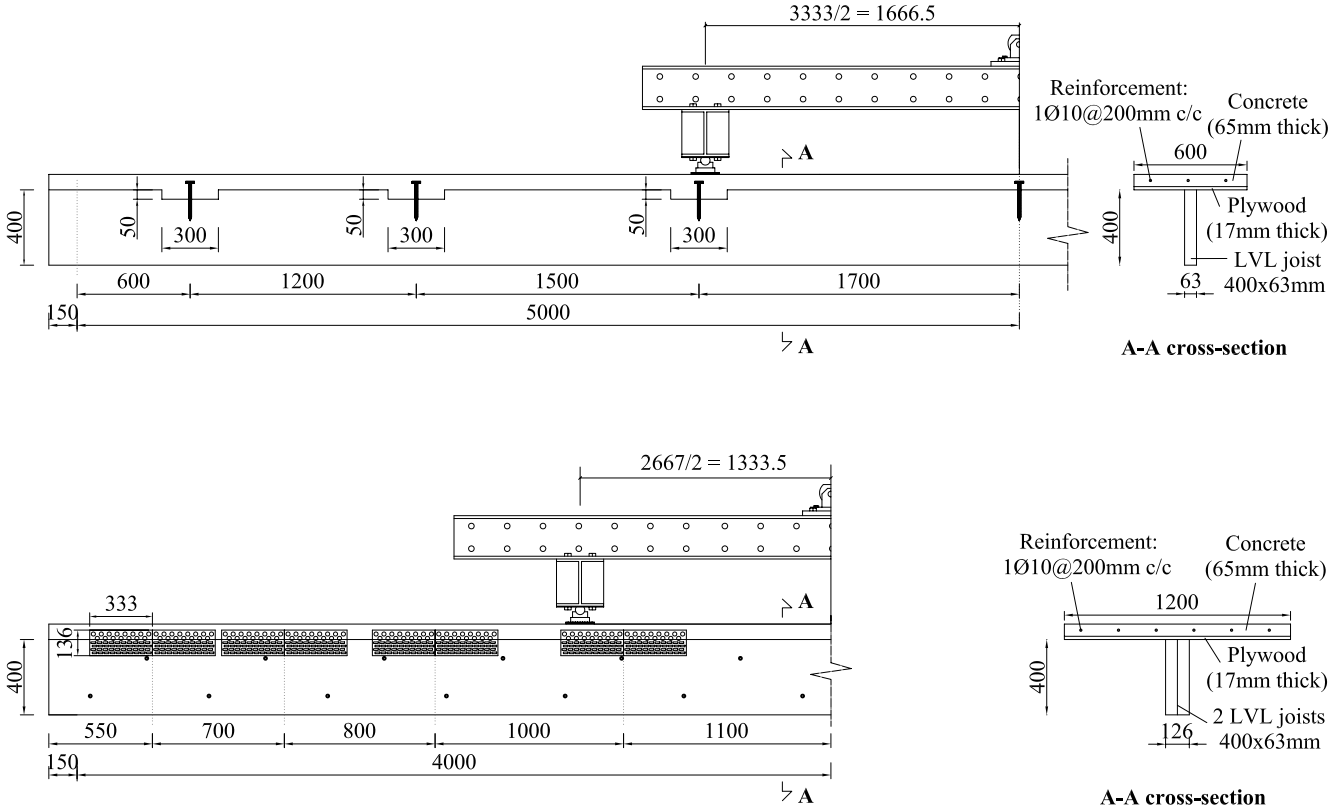

Fig. 4. Elevation and cross section of Beam E1 (top) and Beam F1 (bottom); dimensions in mm (data from Yeoh 2010; Yeoh et al. 2011a)

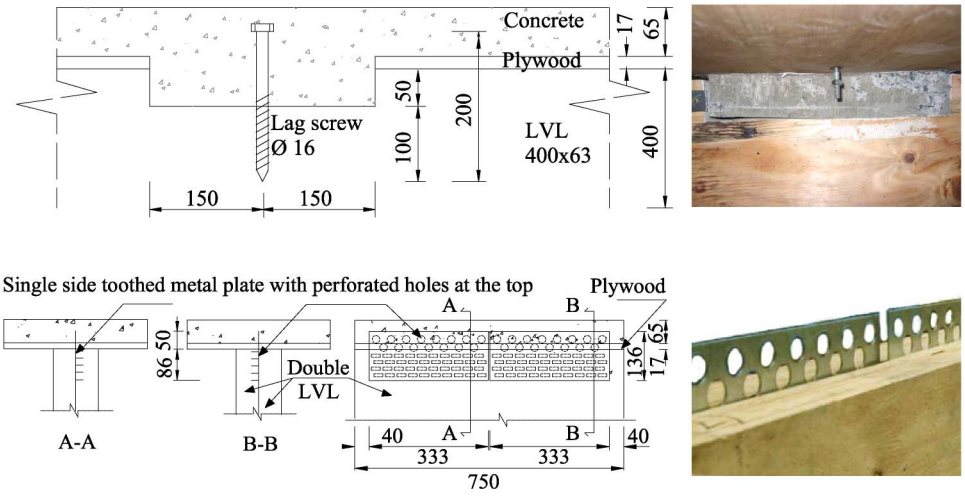

Fig. 5. Details (top left) and photograph (top right) of the notched connection approaching failure (note the concrete crushing on the right-hand side), and details (bottom left) and photograph (bottom right) of the toothed metal plate connection (dimensions in mm) (data from Yeoh 2010)

the length increases. The experimental tests provide the following results: $\mu_{f_t} = 42.67$ MPa and $\text{COV}_{f_t} = 12.8\%$ for 31 specimens (610 mm long); $\mu_{f_t} = 40.74$ MPa and $\text{COV}_{f_t} = 17.4\%$ for 79 specimens (945 mm long); $\mu_{f_t} = 38.03$ MPa and $\text{COV}_{f_t} = 10.3\%$ for 32 specimens (2,438 mm long); and $\mu_{f_t} = 37.02$ MPa and $\text{COV}_{f_t} = 13.3\%$ for 29 specimens (3,048 mm long). Another experimentally derived equation developed by the New Zealand LVL producer is used to estimate the tensile strengths $\mu_{f_t} = 33.38$ MPa and $\mu_{f_t} = 32.71$ MPa for the beams that are 8 and 10 m long, respectively. For both beams, $\text{COV}_{f_t} = 17.4\%$ (i.e., the largest COV among the various sample lengths) is conservatively assumed.

Because the LVL beam in the tested composite beams is subjected to a combination of bending and tension, its strength depends on both the bending and tensile strength. The interaction between bending and tension is considered in this study using the resistance criteria for combined bending and axial tension provided by Eurocode 5 (CEN 2004b):

$$\frac{\sigma_b}{f_b} + \frac{\sigma_t}{f_t} \leq 1 \tag{6}$$

where σ_b = flexural component of the stress and σ_t = tensile component of the stress.

This inequality can be manipulated to express it in terms of the maximum stress $\sigma_{\max}$ in the bottom fiber of the timber joist:

$$\sigma_{\max} = \sigma_b + \sigma_t \leq f_{MN} = \frac{1 + \frac{\sigma_t}{\sigma_b}}{\frac{f_t}{f_b} + \frac{\sigma_t}{\sigma_b}} f_t \tag{7}$$

The stress ratio σ_t/σ_b depends on the ratio M/N between the bending moment M and the axial force N in the timber joist, which is affected by the stiffness ratio between the reinforced concrete slab and timber joist, as well as by the stiffness of the connection system. Thus, this ratio is not known a priori. However, if the simplified gamma method in Annex B of Eurocode 5 (CEN 2004b) is used to investigate the stress distribution in the composite beam, the values of σ_t/σ_b for Beam Specimens E1 and F1 are 0.906 and 0.885, giving a resulting strength f_{MN} of 38.9 and 39.4 MPa, respectively, and $\text{COV}_{f_{MN}}$ is conservatively assumed equal to the maximum between COV_{f_b} and COV_{f_t}; i.e., $\text{COV}_{f_{MN}} = 17.4\%$ (Table 1). The correlation between f_{MN} and E_b is assumed equal to the correlation between f_b and E_b; i.e., $\rho_{f_{MN}E_b} = 0.59$.

Characterization of the Material Parameters of the Concrete Topping

The values of the concrete compression strength, f_c, were measured from a number of cylinders at 7 days, 28 days, and at the time of beam testing; i.e., about 5 months after casting (Yeoh 2010). On the test day, six concrete samples were tested for Beam E1, giving $\mu_{f_c} = 48.17$ MPa and $\text{COV}_{f_c} = 3.51\%$; and two concrete samples were tested for Beam F1 (with measured values of $f_c = 52.28$ and 56.48 MPa, respectively), giving $\mu_{f_c} = 54.38$ MPa. In this second case, $\text{COV}_{f_c} = 10\%$ is conservatively assumed. The mean value of the concrete elastic modulus, E_c, is derived using the indications in Eurocode 2 (CEN 2004a), and COV_{E_c} is assumed equal to COV_{f_c} (Table 1). The correlation between f_c and E_c is assumed to be equal to 0.8.

The constitutive model of the reinforcement steel in the concrete topping is described by the yield stress, f_y, and Young's modulus, E_s. Because specific coupon testing of the reinforcement steel was not performed in the experimental program at the University of Canterbury, the statistical properties of the constitutive parameters are assumed here as follows: $\mu_{f_y} = 525$ MPa (equal to the nominal yield stress), $\mu_{E_s} = 210$ GPa, $\text{COV}_{f_y} = 0.106$, $\text{COV}_{E_s} = 0.033$, and $\rho_{f_yE_s} = 0$ (i.e., f_y and E_s are assumed statistically independent), according to Mirza and MacGregor (1979).

Table 1. Mean Values and COVs of the Material Parameters Assumed as Random Variables

	Beam E1		Beam F1	
Parameter	Mean	COV (%)	Mean	COV (%)
f_{MN} (MPa)	38.90	17.40	39.40	17.40
E_b (MPa)	11,340	7.59	11,340	7.59
f_c (MPa)	48.17	3.51	54.38	10.00
E_c (MPa)	35,258	3.51	36,564	10.00
E_a (MPa)	210,000	3.30	210,000	3.30
f_y (MPa)	525	10.6	525	10.6
$p_{s,\max}$ (kN)	273.62	3.78	278.89	3.39
α (−)	1.1182	21.10	0.7535	19.41
β (1/mm)	2.7116	25.83	3.3939	29.34

Characterization of the Material Parameters of the Shear Connection

The mean values and COVs of parameters $p_{s,\max}$, α, and β are obtained in this study from force-slip curves experimentally recorded during the push-out tests (Yeoh et al. 2011b). Four curves are available for the rectangular notched connectors (Fig. 6), and nine curves are available for the toothed metal plate connectors (Fig. 7). Using a least-squares procedure, the parameters $p_{s,\max}$, α, and β that minimize the error between Eq. (1) and each experimental curve in the range from 0 to 4 mm of slip are determined. Based on these data, the mean values and COVs are computed for the three parameters of each connection type (Table 1). Attention is limited to the 0- to 4-mm slip interval based on preliminary FE analyses, which are used to identify the slip range of variation for the beams considered. In addition, significant degradation of the connection strength is observed in the experimental testing for slips larger than 4 mm. This observation suggests that an ad hoc softening model is needed to describe the shear connection behavior for slip values larger than 4 mm (Yeoh et al. 2011b). This option is not pursued in this work to limit the number of uncertain parameters in the shear connectors. The three parameters $p_{s,\max}$, α, and β are assumed to be statistically independent; i.e., their correlation coefficients are equal to zero. The constitutive curves obtained using the mean values are

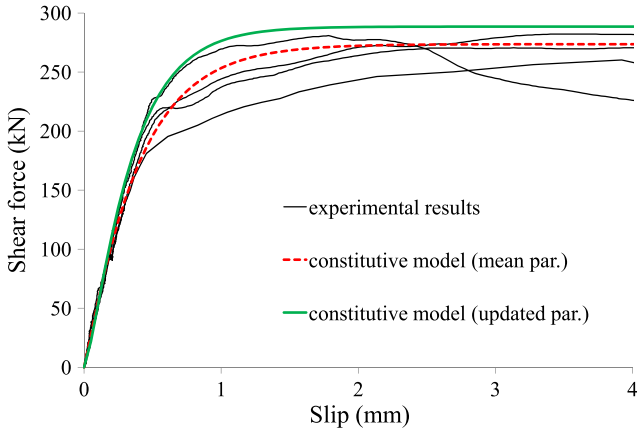

Fig. 6. Identification of the constitutive parameters for rectangular notched connectors (Beam E1)

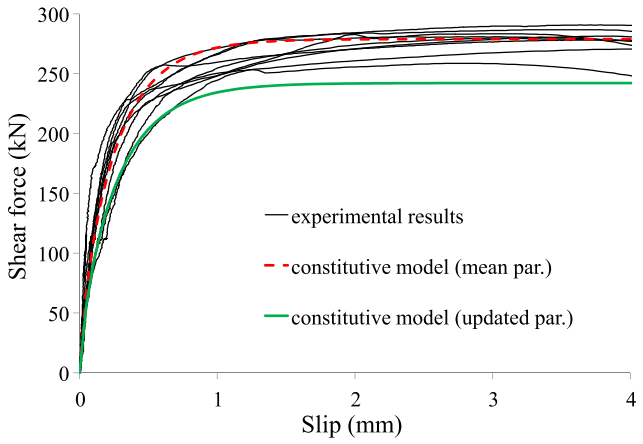

Fig. 7. Identification of the constitutive parameters for toothed metal plate connectors (Beam F1)

Table 2. Values of the Material Parameters in the Updated Models and Variation with Respect to the Initial Mean Values

	Beam E1		Beam F1	
Parameter	Updated	Variation (%)	Updated	Variation (%)
f_{MN} (MPa)	38.2	−1.83	45.4	+15.23
E_b (MPa)	11,340	0.00	11,321	−0.17
f_c (MPa)	48.17	0.00	48.31	−11.16
E_c (MPa)	35,258	0.00	36,345	−0.59
E_a (MPa)	210,000	0.00	210,000	0.00
f_y (MPa)	525	0.00	525	0.00
$p_{s,\max}$ (kN)	288.51	+5.44	242.15	−13.17
α (−)	1.4071	+25.84	0.7491	−0.58
β (1/mm)	3.5069	+29.33	3.1513	−7.15

plotted in Figs. 6 and 7 for the two connection types, respectively. Figs. 6 and 7 also report the constitutive curves obtained using the shear connection parameters of the updated FE models (Table 2) subsequently described in the discussion of the numerical results.

Numerical Modeling

Beams E1 and F1 are discretized into 15 FEs for half of their span length, exploiting the symmetry of the geometry and load configuration. Such discretizations are chosen to model the nonuniform shear connection distribution along the span length, as well as the position of the external load. In the locations corresponding to each rectangular notched connector or toothed metal plate connector, the strength of the connection constitutive model is obtained by smearing the strength of the connectors over the length of the relevant FEs, whereas the strength of the connection constitutive model is set equal to zero elsewhere. Each FE is numerically integrated using five Gauss–Lobatto points in the longitudinal direction and a fiber-discretization in the cross section (20 layers in the concrete and 100 layers in the LVL component). In the probabilistic analysis, each uncertain material parameter is described by a single random variable over the entire structure (i.e., all random fields are assumed with infinite correlation length), as experimental data are insufficient to determine the correlation structure (auto- and cross-correlation functions) for all parameters. In particular, this approach neglects the variability among different shear connectors. The dispersion of the response parameters of a stochastic FE model increases with increasing correlation length of the model parameter random fields; therefore, the estimates of the dispersion of the structural response presented in this study can be considered as upper bounds of the actual response dispersions.

Comparisons between Probabilistic Analysis and Experimental Results

Comparisons between the experimental external load-midspan deflection and the numerical simulations are shown in Fig. 8 (Beam E1) and Fig. 9 (Beam F1). The mean response (μ) and the mean response ± 1 standard deviation ($\mu \pm \sigma$) estimated by the FOSM method are reported. The nonlinear analyses are performed using the Newton–Raphson incremental-iterative procedure with displacement control, using the midspan vertical displacement as the controlled DOF, incremented up to failure with steps of 1 mm. Accordingly, the FOSM method is used to estimate the mean values and the standard deviation of the external load for each assigned deflection increment.

In Beam E1 (Fig. 8), the numerical mean response is in excellent agreement with the experimentally measured response for midspan deflection up to 60 mm, while it presents a slightly smaller

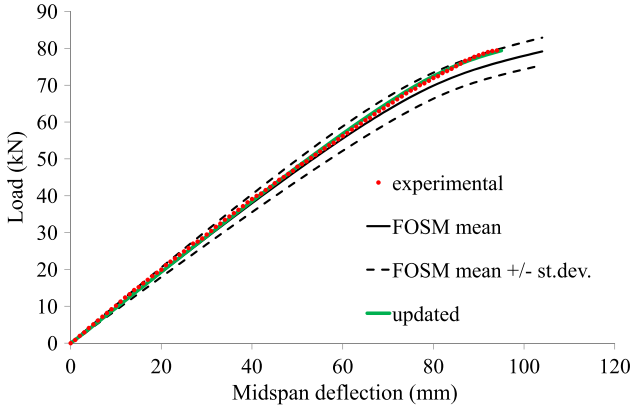

Fig. 8. FOSM, updated model, and experimental load-deflection curves for Beam E1

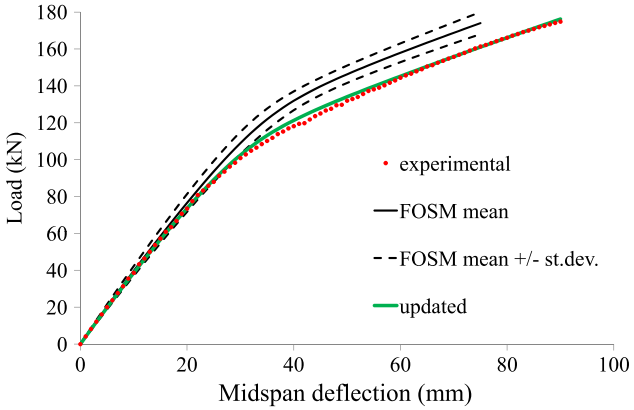

Fig. 9. FOSM, updated model, and experimental load-deflection curves for Beam F1

ultimate load and larger ultimate deflection compared with the experimental results. The experimental results for Beam E1 are always contained between the $\mu - \sigma$ and $\mu + \sigma$ curves. The FOSM-based estimates of the external load at collapse for Beam E1 are $\mu = 79.16$ kN, $\sigma = 3.73$ kN, and COV $= 4.71\%$. In Beam F1 (Fig. 9), the numerical mean response is in excellent agreement with the experimentally measured response for midspan deflection up to 20 mm. For larger deflections, the numerical mean response of Beam F1 presents a delayed stiffness degradation compared with the measured experimental response, resulting in a 16% smaller ultimate deflection and a 0.6% smaller ultimate load compared with the experimental results. In Beam F1, the difference between the experimental result and mean response is larger than 1 standard deviation for midspan deflections larger than 30 mm. The FOSM-based estimates of the external load at collapse for Beam F1 are $\mu = 174.03$ kN, $\sigma = 5.98$ kN, and COV $= 3.44\%$. It is observed that the FOSM-based estimate of the COV of the external load at collapse is very small for both beams. In particular, this COV is considerably smaller than the COV of the LVL strength f_{MN}.

FE Model Updating Results

To understand the reasons for the differences between experimental and numerical load-deflection curves, the FE model updating procedure previously described is used to identify the material parameters' values that ensure the best match between experimentally measured and numerically simulated responses for Beams E1

and F1. The obtained updated FE models provides load-midspan deflection curves that are in excellent agreement with the experimental curves, as shown in Figs. 8 and 9 for Beams E1 and F1, respectively. The corresponding updated parameters are given in Table 2, together with the relevant variations with respect to their estimated mean values. It is observed that the updated model of Beam E1 differs from the initial model mostly in the shear connection parameters. However, these parameter variations are of the same order of magnitude of their standard deviations, as observed by comparing the last three values of the third columns in Tables 1 and 2. This observation is consistent with the result that the load-midspan deflection curve of the updated model of Beam E1 is always contained between the $\mu - \sigma$ and $\mu + \sigma$ curves. At the same time, the updated model of Beam F1 has a significant variation in the strength-related parameters of concrete, LVL, and shear connection. In particular, the updated value of the connection shear strength is 3.9 standard deviations smaller than its estimated mean value. This large discrepancy in the connection shear strength explains the significant discrepancy between the load-midspan deflection curve of the updated model and the model with the parameters set at their mean values.

Validation of FOSM Results through Comparison with MCS Results

The results of the FOSM method are validated through comparisons with MCS analyses, performed for each beam model using 100 (a number usually sufficient for an accurate estimate of mean and standard deviation of the response) and 2,000 (the reference solution) realizations of the set of all random model parameters considered in this study. The material parameters f_{MN} and E_b for the LVL are represented using a lognormal distribution, as recommended in the Australian/New Zealand standard, AUS/NZ 4357.3 (SAA/SANZ 2006). The lognormal distribution is also assumed for the other random material parameters (Melchers 1999). The realizations of the set of all random material parameters are generated using the Nataf model (Ditlevsen and Madsen 1996). Excellent agreement is found between the mean load-midspan deflection curves obtained from the FOSM and MCS analyses (which are not shown in Figs. 8 and 9 for the sake of clarity because they are practically superposed on the FOSM-based mean response curves), while some differences are observed in the estimate of the standard deviation of the external load. Because of space limitations, comparison of the numerical estimates of the standard deviation of the applied force obtained using FOSM and MCS analyses are shown for Beam E1 only. Nonetheless, similar considerations apply to Beam F1 as well. In Beam E1, the FOSM-based response standard deviation is in excellent agreement with the corresponding results obtained using MCS up to deflections corresponding to the first failure in the MCS (i.e., 62 mm for MCS with 100 realizations and 45 mm for MCS with 2,000 realizations), as shown in Fig. 10. In fact, some realizations of the model parameter values in MCS produce FE models that reach failure before the ultimate deflection in the FOSM analysis; i.e., 110 mm. Beyond these midspan deflection values, the results obtained from MCS are conditional to the survival of the FE models obtained from the realizations of the model parameters (i.e., the response statistics are computed excluding the models that are considered as failed when the shear connection reaches its ultimate slip or when the timber component attains its ultimate strain). These conditional results are not directly comparable to the results obtained from FOSM analysis (Barbato et al. 2010). At the ultimate deflection of the FOSM analysis, the failed FE models of Beam E1 are 65 and 1,241 for MCS with 100 and 2,000 realizations, respectively; i.e., 65 and 62% of the total number of samples, respectively.

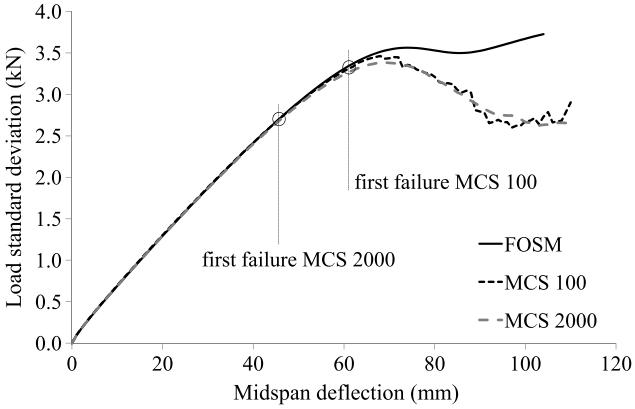

Fig. 10. Estimates of the load standard deviation obtained through FOSM and MCS analyses

Comparisons between Experimental and Numerical Results for Local Response Quantities

Finally, selected results for representative local response quantities are presented in Figs. 11–16. Because the experimentally measured local response results are available as functions of the external load, it is of interest to evaluate the uncertainties in the local response for each assigned load level. Thus, the FE analyses are repeated using the Newton–Raphson incremental-iterative procedure in load-control mode with the external vertical force taken as the controlled load, incremented up to failure with steps of 0.45 kN. In this case, the FOSM-based probabilistic analysis is used to estimate the mean value and standard deviation of the local response quantity considered for each external load increment. Figs. 11 and 12 show the experimental load-slip curves, as well as their numerically simulated results, in which the slip is measured at the first (most external) stud connector in Beam E1 (Fig. 11), and at the midlength of the first toothed metal plate in Beam F1 (Fig. 12), respectively. It is observed that the experimental load-slip curve for Beam E1 is contained almost completely between the mean ± 1 standard deviation FOSM curves. The FOSM mean response describes the experimental results with adequate accuracy only for small values of the slip, while the load-slip curve from the updated model also gives a good estimate of the connection slip at failure. In Beam F1 (Fig. 12), the experimental load-slip curve is contained between the mean ± 1 standard deviation FOSM curves only for small

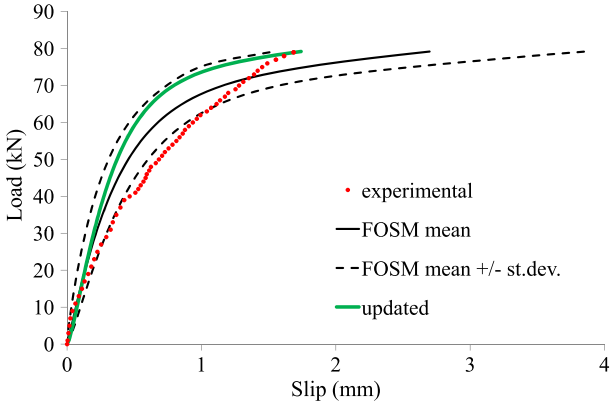

Fig. 11. FOSM, updated model, and experimental load-slip curves at the first connector location of Beam E1

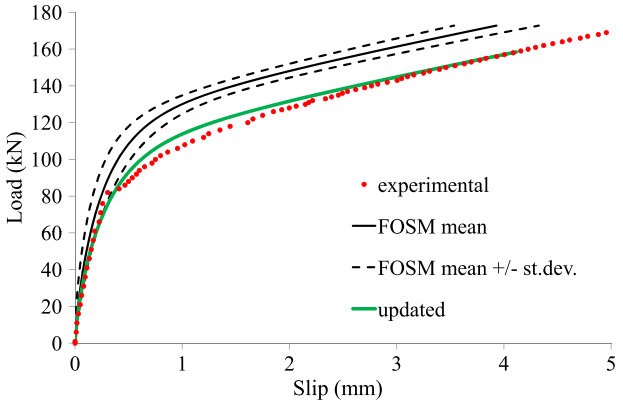

Fig. 12. FOSM, updated model, and experimental load-slip curves at the first connector location of Beam F1

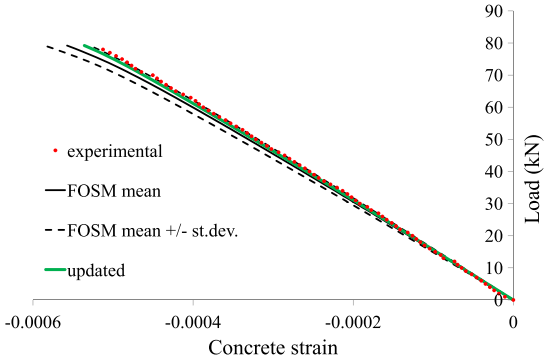

Fig. 13. FOSM, updated model, and experimental load-strain curves in the top fiber of the concrete slab at midspan of Beam E1

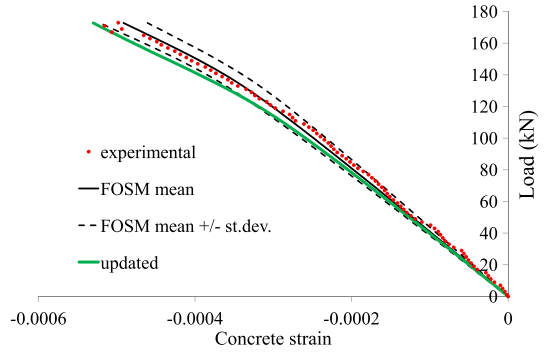

Fig. 14. FOSM, updated model, and experimental load-strain curves in the top fiber of the concrete slab at midspan of Beam F1

values of the slip, while the updated model provides a very good estimate of the experimentally measured slips.

Figs. 13 and 14 depict the experimentally measured and numerically simulated load-strain curves, with the strain measured at the top fiber of the concrete topping in the beam midspan cross section, for Beams E1 and F1, respectively. The discrepancies between experimental tests and numerical simulations are smaller than in the previous case. The updated model shows excellent agreement with the experimental results for Beam E1. In contrast, for Beam F1, the updated model presents an agreement with the experimental results that is slightly worse than the agreement shown by the FE model built using the constitutive parameters' mean values. Figs. 15 and 16 show experimentally measured and numerically simulated load-strain curves, with the strain measured at the bottom fiber of the LVL component in the beam midspan cross section for Beams E1 and F1, respectively. In this case, the experimental load-strain curves are not contained between the mean ± 1 standard deviation FOSM curves, and the updated model does not improve the approximation of the experimentally measured strains compared with the FE model built using the mean values of the material constitutive parameters.

When analyzing the discrepancies between the experimentally measured and numerically simulated local response quantities considered, the following considerations are made. First, the role and importance of uncertainties in the experimental values differs between global and local response quantities, because accurate measurement of very small local quantities (strains and slips) is more difficult to achieve compared with measurement of larger global quantities (deflections). In addition, there are intrinsic limitations on the representation of local quantities when FE frame models are adopted instead of more complex three-dimensional models (for example, using solid/shell FEs). Furthermore, some local response quantities (such as the slip at the concrete-timber interface) are affected by physical phenomena (such as bond and friction) that are not modeled by the frame FEs used in this

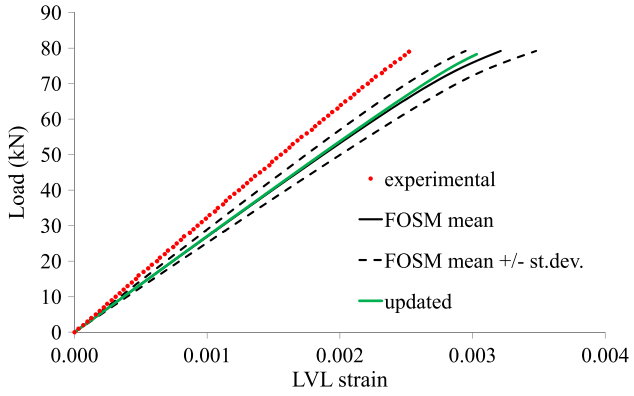

Fig. 15. FOSM, updated model, and experimental load-strain curves in the bottom fiber of the LVL beam at midspan of Beam E1

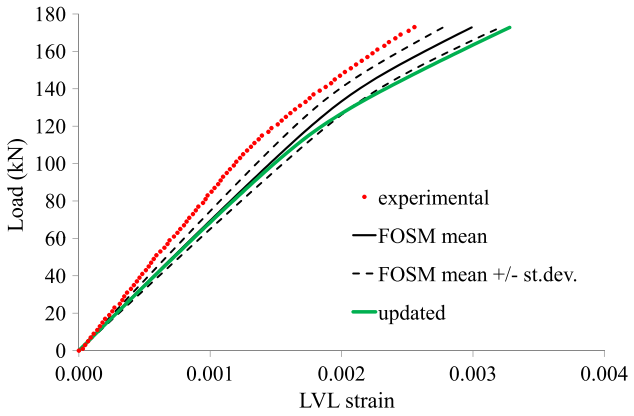

Fig. 16. FOSM, updated model, and experimental load-strain curves in the bottom fiber of the LVL beam at midspan of Beam F1

paper. Finally, there are discrepancies between the actual stress state of the materials and connectors in the beams and the stress state in the block specimens used to identify the constitutive parameters of the connection (Yeoh et al. 2011b). These discrepancies could possibly explain the differences (observed in Figs. 6 and 7) between the experimental shear-slip curves and the constitutive shear-slip model defined by the parameters obtained through FE model updating. Based on these considerations, it can be concluded that the agreement observed between experimentally measured and numerically simulated local response quantities is very good, given the limits of the FE models used in this research.

Discussion on Prospective Design Applications

This study illustrates an efficient integration of a nonlinear FE beam model and a simplified probabilistic response analysis methodology. This integration has several prospective design applications that are based on the uncertainty quantification in the structural performance of timber-concrete composite beams.

In fact, the proposed integrated computational tool can be effectively used for the assessment and design of timber-concrete composite beams because it can realistically account for the effects of material nonlinearity and material parameter variability. In addition, this FE model, extended with FE response sensitivity analysis capabilities, represents an ideal tool for the calibration of the partial resistance factors needed; e.g., in load and resistance factor design (AASHTO 2004) and in limit state design (e.g., CEN 2002). The calibration of the partial resistance factors requires the repeated solution of a nonlinear structural reliability problem; e.g., using the first-order reliability method (FORM) (Melchers 1999). FORM involves the identification of the so-called design point (i.e., the most likely failure point), which is commonly obtained by solving a nonlinear constrained optimization problem through iterative gradient-based numerical optimization algorithms. The availability of accurate and consistent FE response sensitivities greatly improves the convergence rate of these algorithms.

The proposed integrated computational tool also can be used to investigate specific issues related to the analysis and design of timber-concrete composite structures; e.g., the significant discrepancies found between the values of the material parameters describing the shear connections obtained from statistical analysis of coupon testing and from the FE model updating procedure. These discrepancies suggest that the mechanical conditions experienced by the shear connection during coupon testing and during loading of the structural component are somewhat different, especially for toothed metal plate connectors. As a consequence, the results presented in this study suggest that there could be a need to develop appropriate correlation relationships to modify the values of the connection parameters obtained from coupon testing into the values to be used for design and assessment purposes. To support these studies, further experimental tests including several identically built timber-concrete composite beams are recommended to directly evaluate the response variability and identify other potential issues that may have significant effects on the performance of this structural typology.

It is noteworthy that the approach presented in this paper can be extended to probabilistic time-dependent response analysis; provided that suitable time-dependent constitutive laws are adopted to model the long-term material behavior and that the statistical characterizations (mean values, COVs, and correlation coefficients) of the required model parameters are available. Thus, an important prospective application of this approach is its extension to the assessment and design of timber-concrete composite beams under long-term service conditions.

Conclusions

A nonlinear FE beam model with deformable shear connection is used in conjunction with a methodology for probabilistic response analysis, the mean-centered FOSM method. The FOSM method accounts for the uncertainties in the parameters describing the constitutive models of timber, concrete, and shear connectors. In addition, a FE model updating procedure is used to identify the material parameters' values that ensure the best match between experimentally measured and numerically simulated response. The benchmark problems considered are LVL-concrete composite beams for which experimental results up to failure, as well as tests on specimens of LVL, concrete, and connectors, are available.

The first objective of this study is the evaluation of the variability of global and local structural response quantities that result from the uncertainties in the constitutive parameters of timber, concrete, and shear connectors. The results presented in the paper show that the variability of the beam capacity owing to the uncertainty in the material parameters is very small, particularly when compared with the variability of the LVL strength f_{MN}. It is shown that the adopted sensitivity-based FOSM method for probabilistic analysis is a fairly simple and computationally efficient tool for assessing the influence of uncertainties on the nonlinear response of timber-concrete composite structures. Very good agreement is found between FOSM and the computationally more expensive MCS.

The second objective of this study is to analyze the correlation between the experimental measurements and numerical results based on FE models, with the values of the constitutive parameters set equal to their mean values as identified in experimental testing, and equal to the optimized values obtained through a FE model updating procedure, respectively. The results presented in this paper show that the uncertainties of the constitutive parameters of LVL, concrete, and shear connectors have a significant influence on the correlation between experimental and numerical results. Most of the experimental results fall within the numerically predicted mean ± 1 standard deviation of the response quantity considered. In other cases, the differences between the numerical and experimental results are larger than 1 standard deviation of the response quantity being examined. In both situations, the optimal values of the constitutive parameters (obtained using the FE model updating procedure described in the paper) show variations with respect to their mean values that may exceed their COV. These results suggest that the FE model adopted in this study is adequate to describe the main aspects of the short-term structural behavior of timber-concrete composite beams. However, the uncertainties in the identification of the constitutive parameters from experimental testing are a crucial issue in the definition of an accurate nonlinear FE model for timber-concrete composite structures.

Acknowledgments

The writers would like to acknowledge Mr. Hank Bier (Rotorua, New Zealand) for all of the information provided on the mechanical properties of LVL; Dr. David Yeoh (Universiti Tun Hussein Onn, Malaysia) for providing the experimental data of the composite beams tested in New Zealand, as well as the mechanical properties of the concrete and connection systems used in the same composite beams; and Ms. Melissa G. Schultz for the help kindly provided in proofreading the manuscript. The writers gratefully acknowledge partial support of this research by the LSU Council on Research

through the 2009–2010 Faculty Research Grant Program; the Longwell's Family Foundation through the Fund for Innovation in Engineering Research (FIER) Program; and the Louisiana Board of Regents (LA BoR) through the Louisiana Board of Regents Research and Development Program, Research Competitiveness (RCS) subprogram under Award No. LESQSF(2010-13)-RD-A-01. Any opinions, findings, conclusions, or recommendations expressed in this publication are those of the writers and do not necessarily reflect the views of the sponsors.

References

AASHTO. (2004). *LRFD bridge design specifications*, AASHTO, Washington, DC.

Balogh, J., Fragiacomo, M., Gutkowski, R. M., and Fast, R. S. (2008). "Influence of repeated and sustained loading on the performance of layered wood-concrete composite beams." *J. Struct. Eng.*, 134(3), 430–439.

Barbato, M., and Conte, J. P. (2005). "Finite element response sensitivity analysis: A comparison between force-based and displacement-based frame element models." *Comput. Methods Appl. Mech. Eng.*, 194(12-16), 1479–1512.

Barbato, M., Gu, Q., and Conte, J. P. (2010). "Probabilistic push-over analysis of structural and soil-structure systems." *J. Struct. Eng.*, 136(11), 1330–1341.

Barbato, M., Zona, A., and Conte, J. P. (2007). "Finite element response sensitivity analysis using three-field mixed formulation: General theory and application to frame structures." *Int. J. Numer. Methods Eng.*, 69(1), 114–161.

Baruch, M. (1982). "Methods of reference basis for identification of linear dynamic structures." *Proc., 23rd Structures, Structural Dynamics and Materials Conf., New Orleans, May*, AIAA, New York.

Bathon, L., Bletz, O., and Schmidt, J. (2006). "Hurricane proof buildings—an innovative solution using prefabricated modular wood-concrete-composite elements." *Proc., 9th World Conf. on Timber Engineering*, Portland, OR (CD-ROM).

Ceccotti, A. (2002). "Composite concrete-timber structures." *Prog. Struct. Eng. Mater.*, 4(3), 264–275.

Ceccotti, A., Fragiacomo, M., and Giordano, S. (2007). "Long-term and collapse tests on a timber-concrete composite beam with glued-in connection." *Mater. Struct.*, 40(1), 15–25.

Conte, J. P., Barbato, M., and Spacone, E. (2004). "Finite-element response sensitivity analysis using force-based frame models." *Int. J. Numer. Methods Eng.*, 59(13), 1781–1820.

Conte, J. P., Vijalapura, P. K., and Meghella, M. (2003). "Consistent finite-element response sensitivity analysis." *J. Eng. Mech.*, 129(12), 1380–1393.

Dall'Asta, A., and Zona, A. (2002). "Non-linear analysis of composite beams by a displacement approach." *Comput. Struct.*, 80(27–30), 2217–2228.

Dall'Asta, A., and Zona, A. (2004). "Slip locking in finite elements for composite beams with deformable shear connection." *Finite Elem. Anal. Des.*, 40(13–14), 1907–1930.

Dall'Asta, A., and Zona, A. (2005). "Finite element model for externally prestressed composite beams with deformable connection." *J. Struct. Eng.*, 131(5), 706–714.

Dias, A. M. P. G., Lopes, S. M. R., Van de Kuilen, J. W. G., and Cruz, H. M. P. (2007). "Load-carrying capacity of timber-concrete joints with dowel-type fasteners." *J. Struct. Eng.*, 133(5), 720–727.

Ditlevsen, O., and Madsen, H. O. (1996). *Structural reliability methods*, Wiley, New York.

Edlund, B. (1995). "Tension and compression." *Timber engineering, step 1*, 1st Ed., Centrum Hout, Netherlands, B2/1–B2/8.

European Committee for Standardization (CEN). (2002). "Eurocode 0: Basis of structural design." *EN 1990*, Brussels.

European Committee for Standardization (CEN). (2004a). "Eurocode 2: Design of concrete structures. Part 1.1: General—general rules and rules for buildings." *EN 1992-1-1*, Brussels.

European Committee for Standardization (CEN). (2004b). "Eurocode 5: Design of timber structures. Part 1.1: General—common rules and rules for buildings." *EN 1995-1-1*, Brussels.

Fragiacomo, M. (2005). "A finite element model for long-term analysis of timber-concrete composite beams." *Struct. Eng. Mech.*, 20(2), 173–189.

Fragiacomo, M. (2006). "Long-term behavior of timber-concrete composite beams. II: Numerical analysis and simplified evaluation." *J. Struct. Eng.*, 132(1), 23–33.

Fragiacomo, M., Amadio, C., and Macorini, L. (2004). "A finite element model for collapse and long-term analysis of steel-concrete composite beams." *J. Struct. Eng.*, 130(3), 489–497.

Fragiacomo, M., and Ceccotti, A. (2006). "Long-term behavior of timber-concrete composite beams. I: Finite element modeling and validation." *J. Struct. Eng.*, 132(1), 13–22.

Friswell, M. I., and Mottershead, J. E. (1995). *Finite element model updating in structural dynamics*, Kluwer Academic, Dordrecht, Netherlands.

Gutkowski, R., Brown, K., Shigidi, A., and Natterer, J. (2008). "Laboratory tests of composite wood-concrete beams." *Constr. Build. Mater.*, 22(6), 1059–1066.

Gutkowski, R. M., Miller, N., Fragiacomo, M., and Balogh, J. (2011). "Composite wood-concrete beams using utility poles: Time-dependent behavior." *J. Struct. Eng.*, 137(6), 625–634.

Haftka, R. T., and Gurdal, Z. (1993). *Elements of structural optimization*, Kluwer, Dordrecht, Netherlands.

Haukaas, T., and Der Kiureghian, A. (2004). "Finite element reliability and sensitivity methods for performance-based engineering." *Rep. PEER 2003/14*, Pacific Earthquake Engineering Research Center, Univ. of California at Berkeley, Berkeley, CA.

Haukaas, T., and Der Kiureghian, A. (2005). "Parameter sensitivity and importance measures in nonlinear finite-element reliability analysis." *J. Eng. Mech.*, 131(10), 1013–1026.

Jaishi, B., Kim, H. J., Kim, M. K., Ren, W. X., and Lee, S. H. (2007). "Finite element model updating of concrete-filled steel tubular arch bridge under operational condition using modal flexibility." *Mech. Syst. Signal Process.*, 21(6), 2406–2426.

Kleiber, M., Antunez, H., Hien, T. D., and Kowalczyk, P. (1997). *Parameter sensitivity in nonlinear mechanics: Theory and finite element computation*, Wiley, New York.

Lukaszewska, E., Fragiacomo, M., and Johnsson, H. (2010). "Laboratory tests and numerical analyses of prefabricated timber-concrete composite floors." *J. Struct. Eng.*, 136(1), 46–55.

MathWorks. (2010a). *MATLAB 7 getting started guide*, MathWorks, Natick, MA.

MathWorks. (2010b). *Optimization toolbox 5 user's guide*, MathWorks, Natick, MA.

Melchers, R. E. (1999). *Structural reliability analysis and predictions*, 2nd Ed., Wiley, Chichester, United Kingdom.

Mirza, S. A., and MacGregor, J. G. (1979). "Variability of mechanical properties of reinforcing bars." *J. Struct. Div.*, 105(5), 921–937.

Mottershead, J. E., and Friswell, M. I. (1993). "Model updating in structural dynamics: A survey." *J. Sound Vib.*, 167(2), 347–375.

Newmark, N. M., Siess, C. P., and Viest, I. M. (1951). "Tests and analysis of composite beams with incomplete interaction." *Proc. Soc. Exp. Stress Anal.*, 9(1), 75–92.

Ollgaard, J. G., Slutter, R. G., and Fisher, J. W. (1971). "Shear strength of stud connectors in lightweight and normal weight concrete." *AISC Eng. J.*, 8(2), 55–64.

Saenz, L. P. (1964). "Discussion of 'Equation for the stress-strain curve of concrete' by P. Desayi and S. Krishnan." *ACI J.*, 61(9), 1229–1235.

Schänzlin, J. (2003). "Time dependent behavior of composite structures of board stacks and concrete." Ph.D. thesis, Univ. of Stuttgart, Stuttgart, Germany (in German).

Standards Association of Australia /Standards Association of New Zealand (SAA/SANZ). (2006). "Structural laminated veneer lumber (LVL). Part 3: Determination of structural properties—Evaluation methods." *AUS/NZ 4357.3:2006*, Sydney, Australia.

To, L., Fragiacomo, M., Balogh, J., and Gutkowski, R. M. (2011). "Long-term load test of a wood-concrete composite beam." *Proc. Inst. Civ. Eng. Struct. Build.*, 164(2), 155–163.

Wei, F. S. (1990). "Structural dynamic model improvement using vibration test data." *AIAA J.*, 28(1), 175–177.
Yeoh, D. (2010). "Behavior and design of timber-concrete composite floor systems." Ph.D. thesis, Univ. of Canterbury, Christchurch, New Zealand.
Yeoh, D., Fragiacomo, M., and Deam, B. (2011a). "Experimental behaviour of LVL-concrete composite floor beams at strength limit state." *Eng. Struct.*, 33(9), 2697–2707.
Yeoh, D., Fragiacomo, M., De Franceschi, M., and Buchanan, A. (2011b). "Experimental tests of notched and plate connectors for LVL-concrete composite beams." *J. Struct. Eng.*, 137(2), 261–269.
Yeoh, D., Fragiacomo, M., De Franceschi, M., and Koh, H. B. (2011c). "State of the art on timber-concrete composite structures: Literature review." *J. Struct. Eng.*, 137(10), 1085–1095.
Zhang, Q. W., Chang, T. Y. P., and Chang, C. C. (2001). "Finite-element model updating for the Kap Shui Mun cable-stayed bridge." *J. Bridge Eng.*, 6(4), 285–293.
Zivanovic, S., Pavic, A., and Reynolds, P. (2007). "Finite element modelling and updating of a lively footbridge: The complete process." *J. Sound Vib.*, 301(1-2), 126–145.
Zona, A. (2002). "Finite element modelling of composite beams." Ph.D. thesis, Univ. of Ancona, Ancona, Italy.
Zona, A., Barbato, M., and Conte, J. P. (2005). "Finite element response sensitivity analysis of steel-concrete composite beams with deformable shear connection." *J. Eng. Mech.*, 131(11), 1126–1139.
Zona, A., Barbato, M., and Conte, J. P. (2006). "Finite element response sensitivity analysis of continuous steel-concrete composite girders." *Steel Compos. Struct.*, 6(3), 183–202.
Zona, A., Barbato, M., and Conte, J. P. (2008). "Nonlinear seismic response analysis of steel-concrete composite frames." *J. Struct. Eng.*, 134(6), 986–997.
Zona, A., Barbato, M., Dall'Asta, A., and Dezi, L. (2010). "Probabilistic analysis for design assessment of continuous steel-concrete composite girders." *J. Constr. Steel Res.*, 66(7), 897–905.
Zona, A., and Ranzi, G. (2011). "Finite element models for nonlinear analysis of steel-concrete composite beams with partial interaction in combined bending and shear." *Finite Elem. Anal. Des.*, 47(2), 98–118.